Scaling organization of fracture tectonics (SOFT) and earthquake mechanism

Claude J. Allègre [a,b], Jean Louis Le Mouël [a,*], Ha Duyen Chau [a], Clément Narteau [a]

[a] *Institut de Physique du Globe de Paris, 4, Place Jussieu, 75252 Paris Cedex 05, France*
[b] *Université Paris VII, 2, Place Jussieu, 75252 Paris Cedex 05, France*

Abstract

In this paper we use an energy splitting combined with a renormalization group approach to model the behaviour of a fault zone subject to earthquakes. After developing the formalism we explore through numerical experiments the case of a single domain and the case of several interactive domains. This approach is a link between physical approaches, multiblock approaches (like Burridge–Knopoff) and scaling approaches to earthquakes.

1. Introduction

We argue in this paper that an earthquake is a critical phenomenon which takes place when, in a fault zone, fractures at different scales become coherently self-organized. In the frame of this hypothesis we can build model of earthquakes, using an energy approach and a kind of renormalization group-type technique (Wilson, 1979) which we named a scaling technique (Allègre et al., 1982).

In a previous paper (Allègre and Le Mouël, 1994) we showed, using these techniques, that some major observations in rock mechanics and tectonics such as the sudden appearance of fracture, the brittle–ductile transition, the orientation of macrofractures in various conditions can

be accounted for. However, these first attempts were slightly formal since no energy consideration was introduced into the model.

In the present paper we start with energy considerations and the time evolution of partitioning in connection with the creation of fractures at different scales. The basic assumption that each fault at each scale is embedded in the next one is the corner stone of our approach. This view is supported by field observations (Ambrayseys, 1970; Mattauer, 1976; King, 1983; Sammis et al., 1986; Hirata, 1989; Armijo et al., 1989), rock mechanics experiments (Brace and Bombolakis, 1963; Brace et al., 1966; Tapponnier and Brace, 1976; Scholz, 1990), and the observed scaling law in earthquake statistics (Gutenberg and Richter, 1954; Aki, 1967, 1987; Hanks, 1977); it has been the basis of several approaches using percolation theory (Otsuka, 1972; Chelidze, 1982) and, more recently, renormalization group theory

---

* Corresponding author.

(Allègre et al., 1982; Smalley et al., 1985; Newman et al., 1993).

We build along these lines a model which reproduces several observations about earthquakes: sequences with foreshocks and aftershocks, varieties of occurrence of these two types of phenomena, types of earthquakes, Gutenberg–Richter law.

2. The model

Let us consider a fault zone made of different segments with different geometries, different orientations, different thicknesses of rigid plates, but 'coherently' organized by previous tectonics (Fig. 1). This 'historic polarization' is a fundamental constraint in earthquake modelling (Scholz, 1990; Lockner and Byerlee, 1993; King et al., 1993).

We want to study the seismic behaviour of the fault zone. We define a set of domains along this fault zone, each of which represents a segment or a subsegment, depending on the local tectonic arrangement of the fault and on the local geometry. Each segment is polarized by the existence and orientation of the fault zone and therefore the microfaulting is statistically oriented and organized by such an orientation. The fault zone receives energy continuously from its tectonic environment; this energy is partitioned into the different domains according to the local geological structure. While each domain has its specific behaviour, all of them interact with each other by exchanging energy in various forms between earthquakes or during earthquakes. We study successively the autonomous behaviour of a domain, meaning the response of the domain to the continuous injection of energy, then the interactions between the different domains, and the response of the whole tectonic set.

2.1. Single domain case

2.1.1. Theoretical basis

Let us then consider a single domain (D) of the fault zone which has a given tectonic structure (combination and multiscale distribution of faults, thickness of its brittle part, etc.) and re-
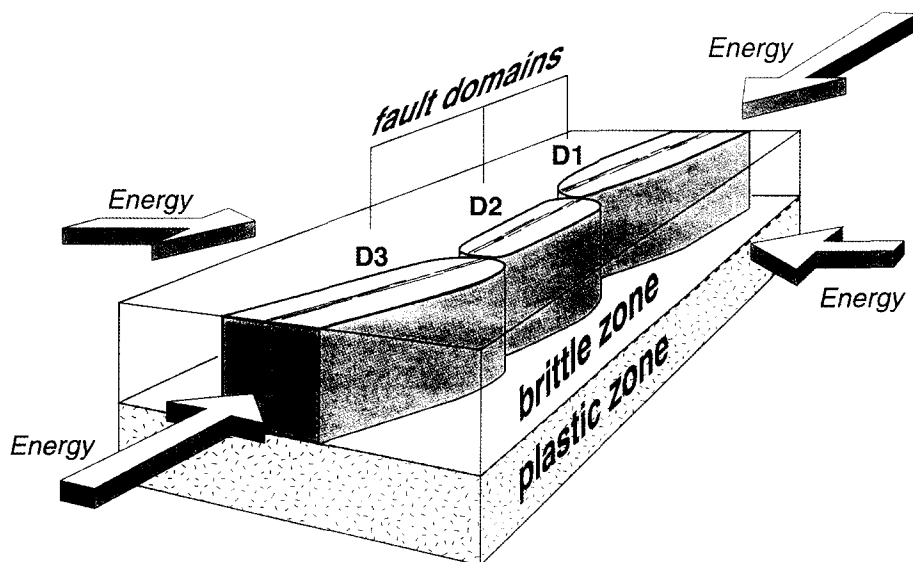

Fig. 1. A fault zone receiving a certain elastic energy resulting from the stress applied to its boundary by plate tectonics is shown. We arbitrarily choose three domains (D_1), (D_2), (D_3). The fault zone is supposed to be composed of a brittle layer above a plastic one. Around each segment, we define a three-dimensional domain with specific geometries, extending to a prescribed depth. The three-dimensional domains are those where the fractures will occur.

ceives energy continuously from plate tectonic movment.

Let $E(t)$ be the energy of the domain (D) at time t. Before an earthquake, the energy E is partitioned into elastic energy and energy for generating and developing cracks. During a period of energy injection we suppose that this partition is not instantaneous but takes a *certain delay time which we choose as the unit of time*. (In a more sophisticated approach the delay time can be considered as a given function of the unit of time, but this will not modify the qualitative behaviour of the model.) This is an important feature of the model and leads us to a *finite difference formalism*.

This quantization is a fundamental characteristic of the model. Δt, which is here given a physical meaning, cannot be reduced to zero. Our model is deliberately intrinsically discrete, and no continuum limit is searched for. In fact, as discussed later, the behaviour of the model depends on the amount of energy injected into (D) during this irreducible elementary time interval.

Let ΔE be the quantum of energy from plate tectonic origin received by (D) in a unit of time (ΔE will be assumed constant)

$$E(t+1) = E(t) + \Delta E \qquad (1)$$

For the sake of simplicity we also consider that the thickness of the brittle zone is uniform throughout (D); and we will consider a two-dimensional (2-D) model.

Let $S(t)$ be the area (volume) of the *sound part* of (D) at time t. When the energy per unit of surface (volume) is larger than a certain quantity ε, the excess energy (per unit area)

$$e_f(t) = \frac{E(t)}{S(t)} - \in = e(t) - \in \qquad (2)$$

can be used to *generate new cracks or develop ancient cracks*. This partitioning of energy is certainly crude, but gives a first approximation.

We use the scaling techniques as in Allègre et al. (1982) and Allègre and Le Mouël (1994). We divide (D) into N elementary domains of order 1 (Fig. 2). At this scale we assume that the probability of nucleating new cracks, during the time

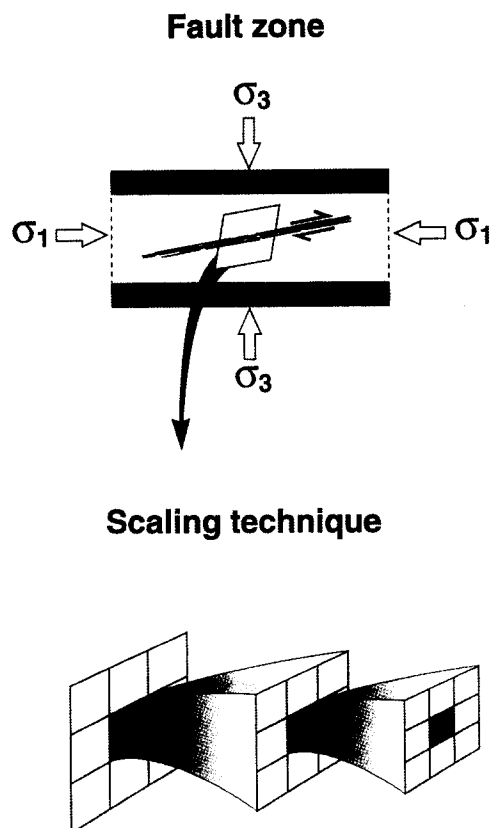**Fault zone**

Scaling technique

Fig. 2. This cartoon illustrates the scaling technique derived from the renormalization group theory used by Allègre and Le Mouël (1994). The domain is divided into subdomains, the subdomains are divided into smaller ones...until the elementary domain scale is reached. We use a grid of 3×3 domains. We define a probability of cracks at the elementary scale (1). With a certain failure criterion, we compute the probability of cracks at scale (2), etc.

interval $(t, t+1)$ is proportionnal to the excess energy $e_f(t)$

$$p_1(t) = \frac{n_1(t)}{N} = K e_f(t) \qquad (3)$$

$n_1(t)$ being the number of squares of order 1 where a crack has been created in the time interval $(t, t+1)$.

We then form $(N/9)$ domains of order 2 comprising (3×3) squares, then $(N/9^2)$ domains of order 3 comprising (3×3) squares of order 2 and so on (Fig. 2). The probability of having new cracks of order 2 by growing small cracks or

$x^3(1-x)^6$

$x^4(1-x)^5$

3 cases   **18 cases**

$x^5(1-x)^4$

$x^6(1-x)^3$

45 cases   **57 cases**

$x^7(1-x)^2$

$x^8(1-x)$

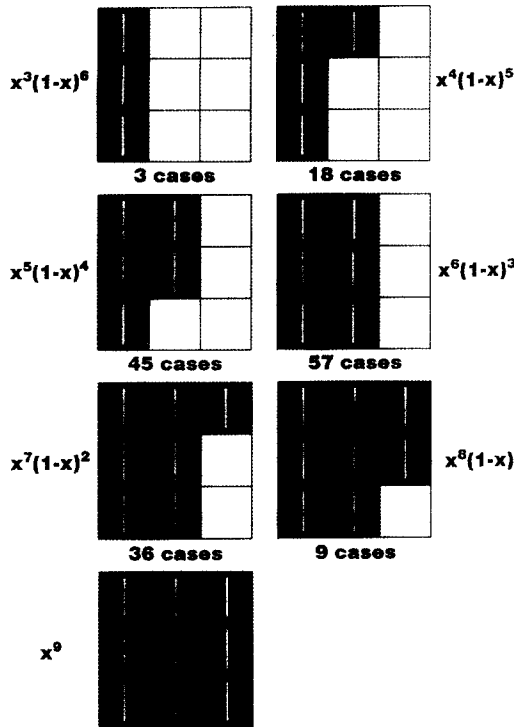**36 cases**   **9 cases**

x^9

Fig. 3. The failure criterion chosen in this paper is quite simple. We suppose a strong polarization of the domains by the fault orientation and therefore consider the creation of cracks more or less in one direction. We suppose that the failure at scale (n) occurs if three squares of order $(n-1)$ are aligned. The graph gives the resultant probabilities and the number of relevant cases. The sum gives the scale transfer polynomial $P(x)$.

propagating the old ones (created in the time interval $(t, t + 1)$) is inferred from the criterium that a square of order 2 is cracked if it contains three cracked squares of order 1 aligned along the fault zone major axis (Fig. 3). Then, as in Allègre and Le Mouël (1994)

$$p_2(t) = P[p_1(t)]$$

with

$$P(x) = 3x^3(1-x)^6 + 18x^4(1-x)^5$$
$$+ 45x^5(1-x)^4 + 57x^6(1-x)^3$$
$$+ 36x^7(1-x)^2 + 9x^8(1-x) + x^9$$

More generally

$$p_k(t) = P[p_{k-1}(t)] \qquad (4)$$

As time increases, energy increases, probabilities of rupture increase following the scaling laws. Eventually, the probability of rupture at different scales converges to generate a critical phenomenon in which rupture occurs coherently at different scales; this event will be defined as an earthquake.

The number of new cracks of order k created during the time interval $(t, t + 1)$ is

$$N_k(t) = p_k(t) \frac{N}{9^{k-1}} \qquad (5)$$

Generation of cracks, at each order, uses energy. This energy is used to increase fracture surface, redistribute strain, emit acoustic waves, and generate heat by friction. If r_k is the amount of energy used to create a crack of order k, the energy used for cracking (D) between times t and $t + 1$ is

$$R(t) = \lambda N \sum_{k=1}^{L(t)} p_k(t) \, r_k \, \frac{1}{9^{k-1}} \qquad (6)$$

λ being a scaling parameter. In the following, we take $r_k = 3^{3k}$, so

$$R(t) = 9\lambda N \sum_{k=1}^{L(t)} p_k^{3^k}$$

This choice means that an 'event' of linear scale d releases an energy proportional to d^3

Note that the energy dissipated in seismic waves, wR with $w \leq 1$, could be computed through the elastic theory of faulting. The energy in domain (D) at time $t + 1$ is then

$$E(t + 1) = E(t) + \Delta E - R(t) \qquad (7)$$

Now, it remains to estimate $S(t + 1)$ in order to compute $e_f(t + 1)$ through Eq. (2) and $p_1(t + 1) \ldots p_k(t + 1)$ through Eqs. (3) and (4). When a critical phenomenon occurs (an earthquake), part of the domain $S(t)$ is broken. This subdomain loses completely its energy which is redistributed in the residual sound part of the domain. The surface $\Delta S(t)$ of the broken subdomains is supposed to be proportional to $R(t)$, the energy lost during earthquakes. The redistribution is not supposed to be instantaneous, but the energy stored in $\Delta S(t)$ is redistributed with a delay, over σ

units of time, at a uniform rate (we take $\sigma \gg 1$ because the action length between different parts of the domain is much longer than the one intervening in the local redistribution). Then the surface bearing the energy $E(t + 1)$ at time $t + 1$ is (Fig. 4)

$$S(t + 1) = S(t) - \mu \sum_{\tau=t}^{\tau=t-\sigma+1} \frac{R(\tau)}{\sigma} \qquad (8)$$

Where μ is a scaling parameter (which could be physically determined). A connected question is the value of the maximum order $L(t)$ reached by fracturing in the time interval $(t, t + 1)$. We assume that $L(t)$ decreases as $S(t)$ decreases according to the relationship

$$L(t) = N_{max} \frac{\log S(t)}{\log S_0} \qquad (9)$$

which means that the maximum surface Σ of the subdomain to be fractured in the time interval $(t, t + 1)$ is proportional to the surface of the remaining sound part of D at t, i.e. $S(t)$ (Σ scales like L^2; S_0 is the value of $S(t)$ at $t = 0$).

Or we may consider that $L(t)$ decreases as the cumulated energy released in previous earthquakes increases

$$L(t) = N_{max} \left[1 - \frac{RI(t - 1)}{A} \right] \qquad (10)$$

with

$$RI(t) = \int_0^t R(\tau) \, d\tau$$

which means that $L(t)$ decreases linearly as the total destroyed surface increases. In fact both Eqs. (9) and (10) lead approximately to the same results. These functions are quite arbitrary and could certainly be improved. However, they do not play a critical role in the following.

2.1.2. Numerical experiment — results

Numerical experiments on models depending on several parameters are difficult to produce. The number of parameters in the present models appears large: K, E_0, ΔE, λ, μ, σ, L_{max}. In fact λ and μ are scaling parameters whose values — which are not independant — could be com-

puted. They play a part in the structure of the series of earthquakes — especially in the mean frequency for K and ΔE given — but not in the onset of the series (while $R(t)$ is small) on which we will focus the discussion later on. The same is the case for the parameter σ (the influence of σ can be seen in the curves $e_f(t)$ of Fig. 5 (a) and (b): a change of slope appears $\sigma \Delta t$ after a big earthquake). We will keep these three parameters constant in the following (see caption of Fig.
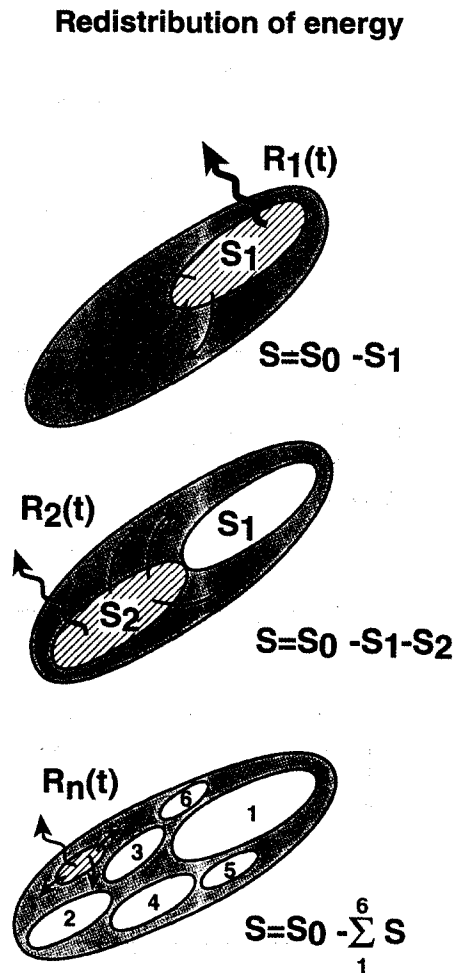
Redistribution of energy

Fig. 4. Redistribution of energy after a critical (or pseudocritical) phenomenon within the domain. Part is lost in the form of tectonic and seismic energy, $R(t)$, another part is redistributed over the part of the domain outside the one where the earthquake occurred; this last part is supposed to lose all its elastic energy.
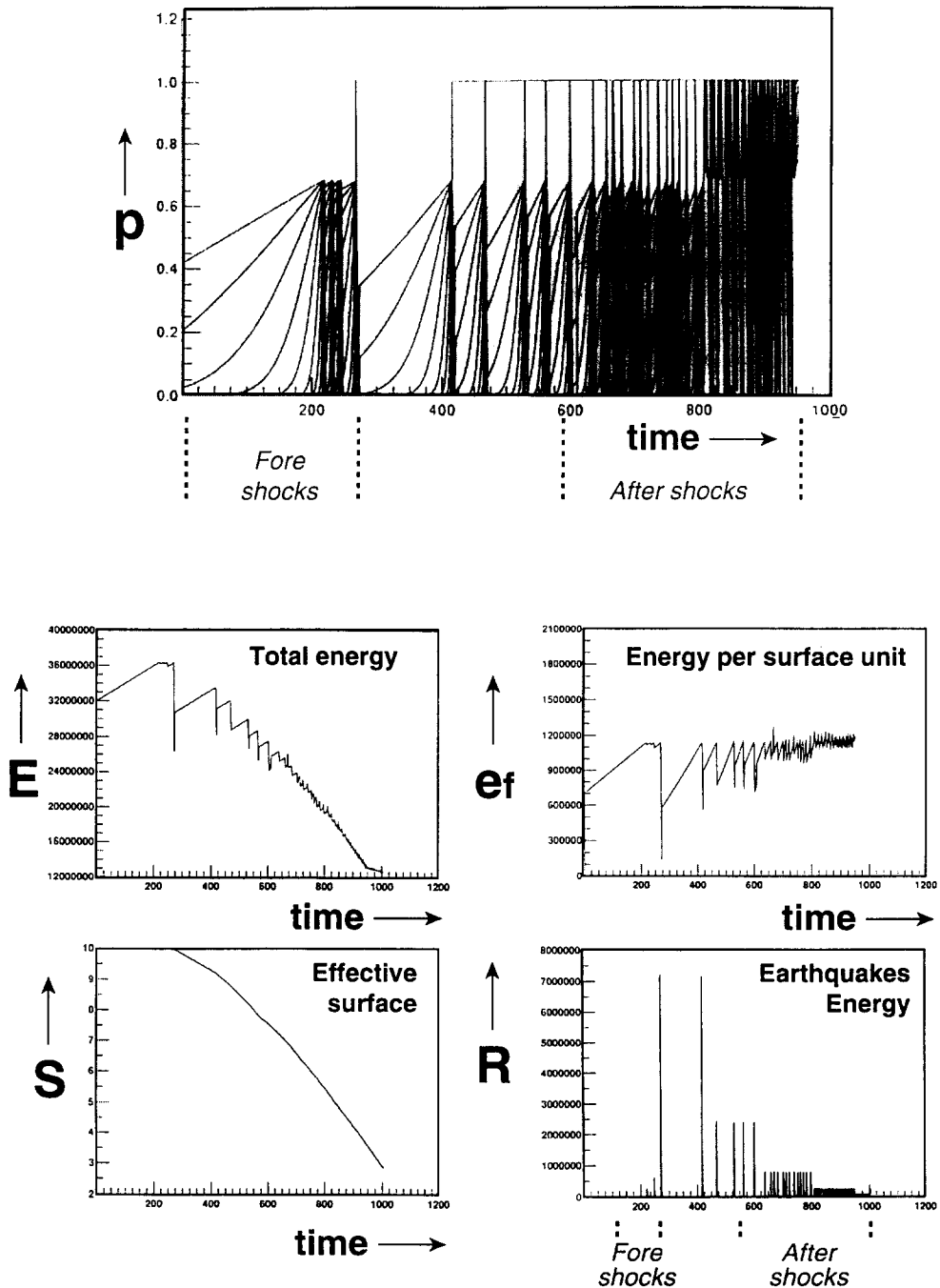
Fig. 5. In (a) and (b) we have represented two numerical experiments. (a) Top: evolution of the probabilities at each scale; note that we have pseudocritical points before a real critical point occurs. Bottom: time variation of E, S (the sound part of the domain), e_f and R. (b) A similar experiment with different values of ΔE and k. In all the numerical experiments presented here the parameters have been given the following values $E_0 = 3.2 \times 10^7$, $S_0 = 10$, $\varepsilon = 2.5 \times 10^6$, $N_{max} = 15$, $\lambda N = 5 \times 10^{-2}$, $\mu = 10^{-7}$, $A = 5$ E_0.

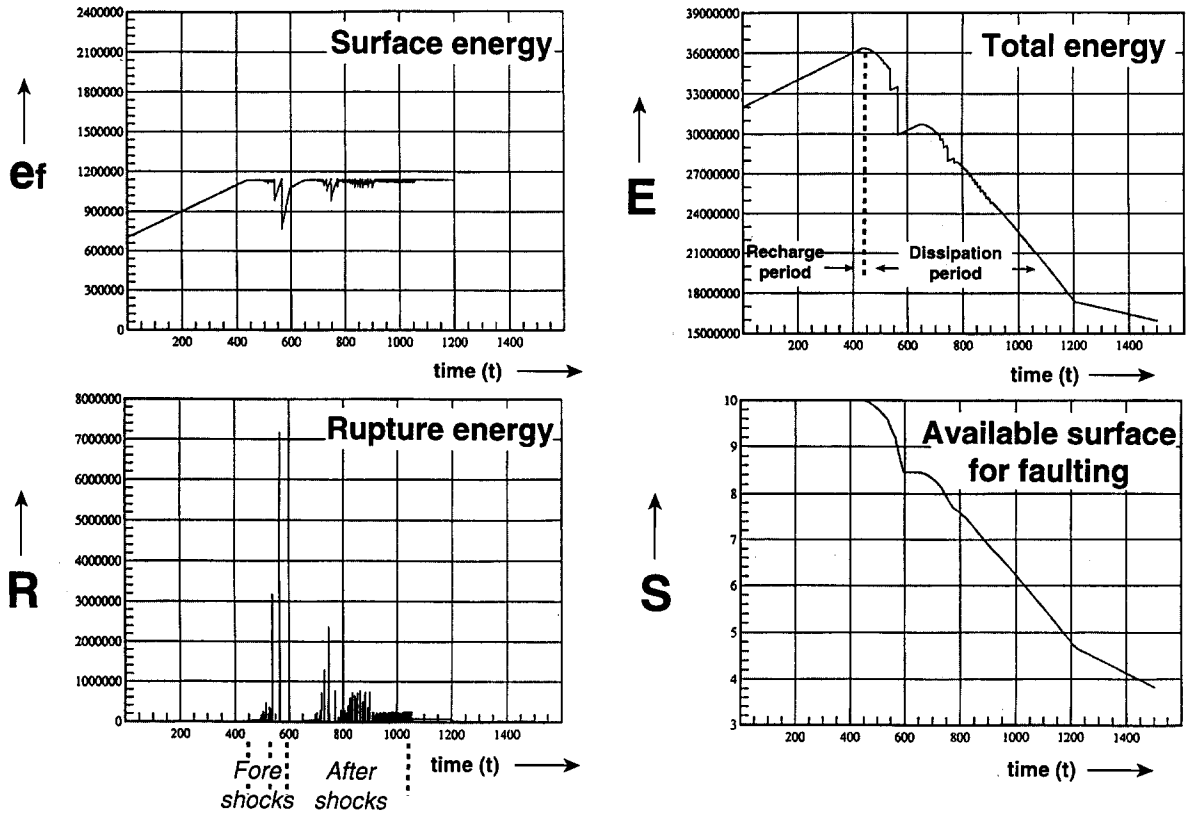**(b)**   **Single domain typical experiment**

Fig. 5 (continued).

5). The parameter ε is also a scaling parameter, changing ε comes down to translating the $p_1(t)$ curve, ε will also be kept constant in the following. We focus the discussion on the parts played by *the parameters* ΔE (the quantum of energy brought to (D) during the unit of time Δt) and K (the proportionality constant relating the probability of creating cracks at level 1 to the excess of unit energy). As we will see, an extremely rich variety of behaviour occurs when varying these two parameters.

2.1.2.1. Typical experiment. As said previously the response time Δt is taken as both the unit of time and the time step. Starting with a given value E_0

of the elastic energy in (D), ΔE is added to E at each time step; the energy per unit surface, the rupture probabilities at all the scales $p_1, p_2, \ldots, p_L$, the energy issued in fractures $R(t)$ are computed at each time step. In the experiment illustrated by Fig. 5, one can see critical points on the curves $p_k(t)$ with corresponding peaks on $R(t)$ interpreted as earthquakes. In fact, we have to distinguish two types of critical points.

(1) True critical points where the probabilities at all different scales converge to a single value; at large scale (14 or 15), the probability curve is a Heaviside function and jumps directly from zero to one, i.e. from no indication of any kind of rupture to complete rupture. This behaviour cor-

responds to a real earthquake where the different scale cracks are coherently organized.

(2) Pseudocritical points where a 'pseudoconvergence' [a] around critical probabilities occurs for scales from 1 to 5 or 6, but not for the higher ones (the corresponding probabilities remain around zero). This corresponds to a large expense of energy but to no large scale rupture. The corresponding little peaks in $R(t)$ are in fact precursor phenomena, foreshocks.

After each peak of $R(t)$, the total energy drops down, so does (E/S), but this last quantity immediately starts rising again owing to the reduction of the active surface S and the redistribution of energy.

The different features of earthquakes are reproduced by our simple model: foreshocks, aftershocks, variability in the rhythm of events and so on. We again point out the difference in nature between foreshocks and aftershocks: — foreshocks are pseudo critical points — aftershocks are mostly real critical points, but with little energy left.

2.1.2.2. Typology.

We have explored the space of the $(K, \Delta E)$ parameters and have been led to distinguish four classes of behaviour, even though the transition from one class to the other is gradual rather than sharp. Those classes correspond to the classification of earthquakes given by Scholz (1990).

(1) Seismic noise. Energy is dissipated in series of small earthquakes separated by silent episodes.

(2) Swarms. Small sequences of earthquakes with almost the same size are separated by silent intervals.

(3) Earthquakes with precursors. The sequence of events is organized around a big peak of $R(t)$ — the main schock. Some small events take place before the big event while other ones, with a time decreasing amplitude, follow it.

(4) Earthquakes without precursors. The big

event occurs suddenly, without any indication of precursors.

2.1.3. Physical interpretation and systematics

As said above, the different types of behaviour of our simple model can be understood by examining the variation of only two parameters: the influence of ΔE, then the influence of the proportionality factor K between p_1 and e_f (Eq. 3).

Let us recall that ΔE is the amount of energy given to the system during the response time Δt taken as the unit of time. This choice makes ΔE depend both on the rate of energy input $\dot{E}$ (in watts) and Δt (in seconds): $\Delta E = \dot{E}\Delta t$. This is to be kept in mind during the discussion. At the beginning of the process the probability of rupture at level 1, as well as E and e_f, grow linearly with time as long as P_1 is smaller than the critical value x_c of the polynomial $P(x)$ $[P(x_c) = x_c]$. Now things depend on the way x_c is approached. If energy is slowly increasing (ΔE small), i.e. if the curve representing $Ke_f(t)$ tends to join the straight line $Ke_f = x_c$ almost tangentially (Figs. 6 and 7(a)), energy is dissipated in small earthquakes (noise or swarm, cases 1 and 2). The reason is that only 'pseudocriticality' is reached, for levels up to 5,6 (in other words the correlation length remains finite). The system remains in a subcritical state.

On the contrary, for larger values of ΔE (the curve $Ke_f(t)$ tends to join the straight line $Ke_f = x_c$ under a larger angle), the two other situations (cases 3 and 4) are met: for intermediate values of ΔE, pseudocritical state can reach several levels up to 6 or 7 before the true critical point is reached ($p_1 > x_c$) — precursors lead to the next earthquake; for larger values of ΔE, p_1 jumps directly from a value significantly smaller than x_c to a value larger than x_c (there is overshoot), and an earthquake occurs without any precursor. During part of the time interval (t, $t + \Delta t$) the system is in a 'supercritical' state.

Up to now the proportionnality constant K (Eq. 3) which links energy to probability of rupture has been assumed constant. But this parameter is also important since it characterizes the local tectonics of the domain. If the domain already contains a lot of faults which can creep, K

---

[a] Pseudoconvergence is the case when probabilities of rupture of low degree are close to the critical probability, but probabilities of high degree are still almost zero.

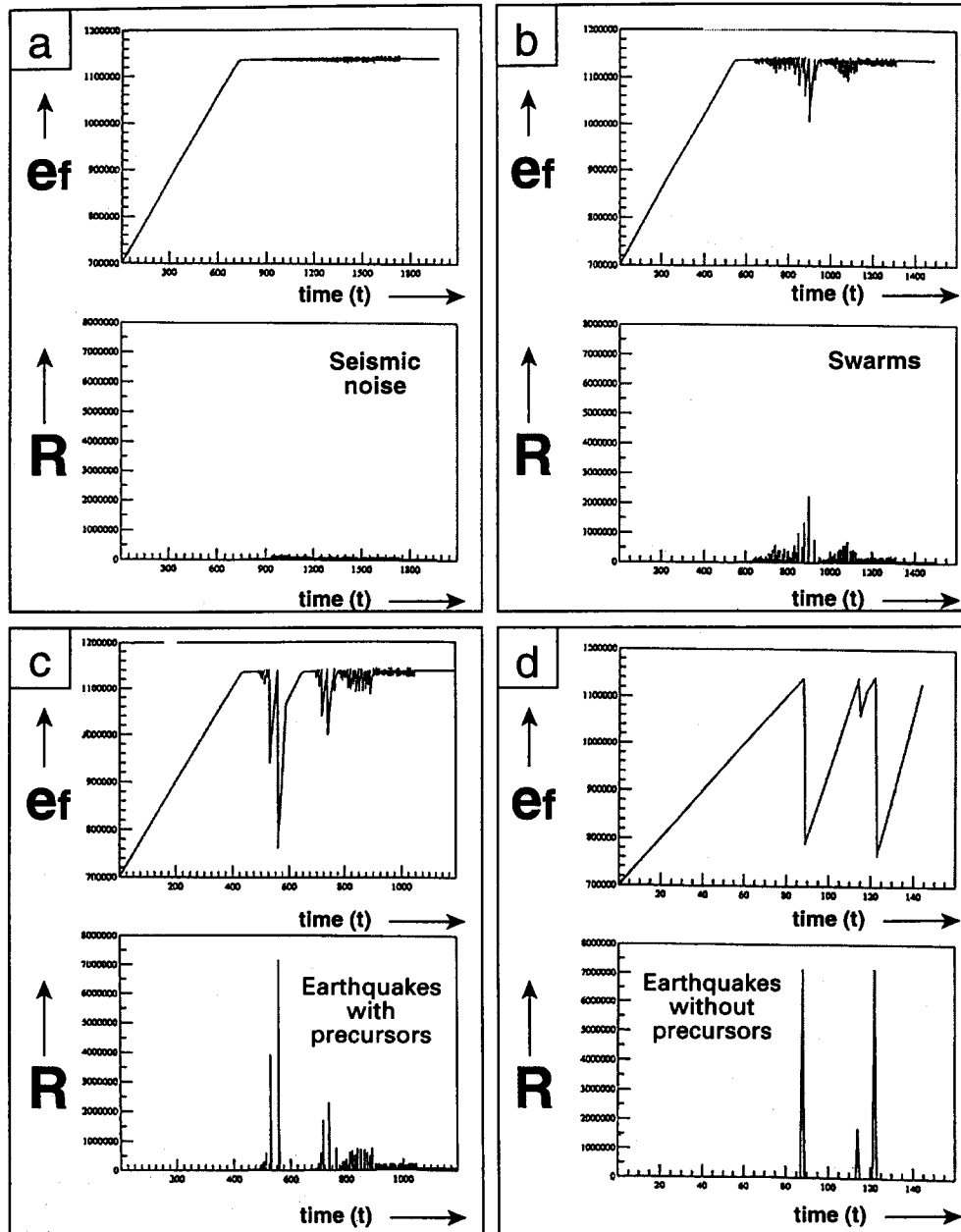# Single domain increase in ΔE

Fig. 6. Types of energy dissipation processes reproduced by our scaling technique. From top to bottom and left to right. Seismic noise which is dissipation of elastic energy by the creation of small cracks without any coherent organization. Swarms which consist of a multiplication of small earthquakes (pseudocritical points) without any big ones. Earthquakes with precursors (foreshocks). Earthquakes without any precursors.

is small; on the other hand, if (D) contains a lot of barriers or asperities (Das and Aki, 1977; Lay and Kanamori, 1981; Aki, 1984), K is high (this simple remark shows that the relationship between p and e_f should not be linear in a realistic model). A systematic study of the $(\Delta E, K)$ space allows us to draw a phase diagram which simply illustrates the different behaviours of the system (Fig. 7(b)). Two main comments can be made about this diagram:

(1) the transitions between noise (a) and swarms (b) are progressive and the boundaries between the different domains of the diagram are in fact rather bands than pure lines;

(2) these boundaries present crenulated (fractal?) features rather than nice differentiable curves. This point will require more thorough examination. This diagram could provide gap theories.

2.1.4. The Gutenberg–Richter statistics

The Gutenberg–Richter law which rules the statistics of the magnitudes of earthquakes appears to be an universal scaling law in seismology (Gutenberg and Richter, 1954; Kanamori and Anderson, 1975). In order to check whether our model satisfies it, we built a number of series earthquakes (series of $R(t)$ as in Fig. 5), computed the cumulated histogram $N(R)$ and drew the corresponding log–log diagram. One example is given in Fig. 8; the slope of the straight line is -0.96. In this example, only the ΔE parameter has been varied — from 6000 to 30 000 by steps of 400, the proportionality constant K (and the other parameters) being kept constant. 'Magnitudes' have been reported on the abscissae axis of the diagram, for comparison with real seismic diagrams (choosing $M = \log R + 1$; in the present paper, we have focused on the time sequence of the events rather than on energy and amplitude scalings; in particular the range of $R(t)$ depends on N_{max} and the form of the polynomial $P(x)$ itself; we will come back to this point in a future work).

2.2. Multidomain case

2.2.1. Theoretical basis

This case is probably closer to reality (Kanamori, 1980; King et al., 1988). The elastic

energy ΔE injected into the fault zone per unit of time is partitioned into $\Delta E_1, \Delta E_2, \ldots, \Delta E_p$, feeding the different domains $D_1, D_2, \ldots, D_p$ according to the tectonic assemblage. The response times $\Delta t_1, \Delta t_2, \ldots, \Delta t_p$ of the different domains are different because of differences in local geology. Complexities (disynchronization) will result since the domains are supposed to exchange energy. In order to avoid the complications resulting from disynchronization we suppose $\Delta t i = \Delta t \forall i$, and, as above, Δt will be the unit of time.

The exchange of energy between the domains takes place in two ways. Elastic (strain) energy is transferred through continuous deformation. Energy is also transferred by the means of acoustic waves emitted by an earthquake or by the sudden faulting associated with it (in other words, a transfer linked with $R(t)$) (Fig. 9). In this first approach we consider the energy transfer between the domains without any delay of time.
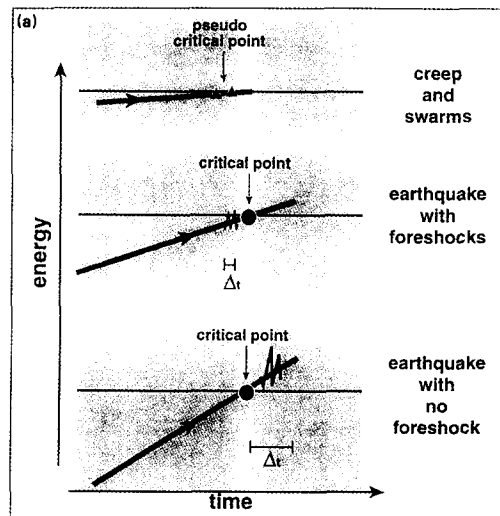

Fig. 7. (a) This is a symbolic explanation of the different behaviours encountered. The horizontal black line represents the critical probability (or critical energy per surface unit). If this energy is approached slowly by the rise of elastic energy, the response is a continuous loss of energy without any real critical phenomena. If the energy increases more quickly, foreshocks (pseudocritical phenomena) lead to a true critical point (a big earthquake). For a steeper increase of energy, the system passes the critical point and a big earthquake takes place directly, without precursors. (b) Phase diagram $(\Delta E, K)$ in semilog. We distinguish five zones: seismic silence, noise, swarms, earthquakes with precursors, earthquakes without precursors.
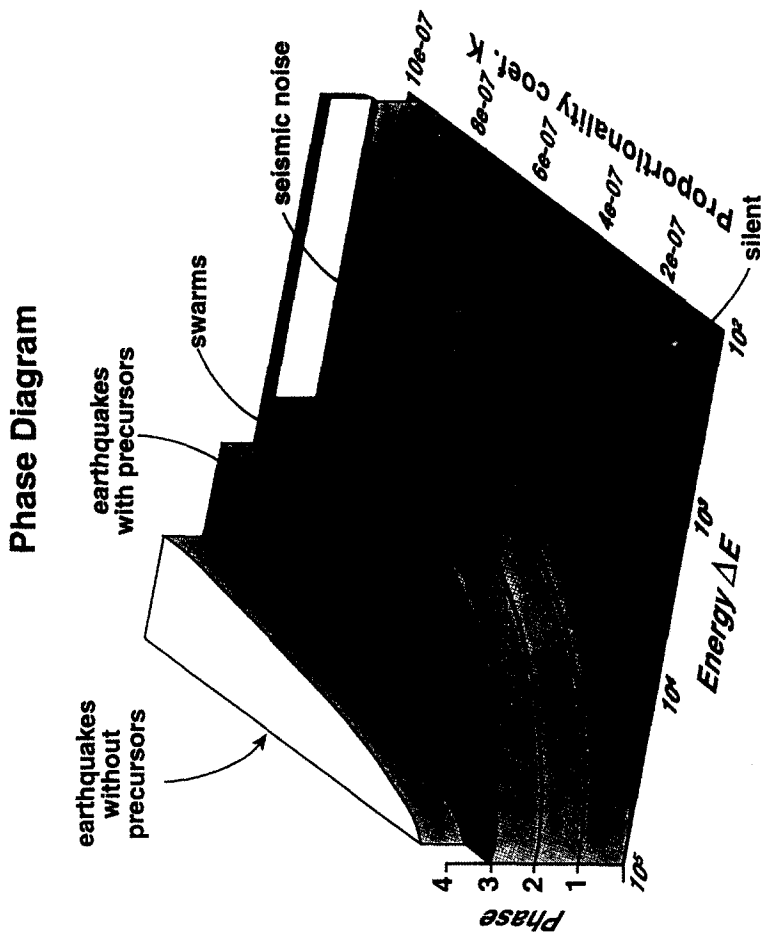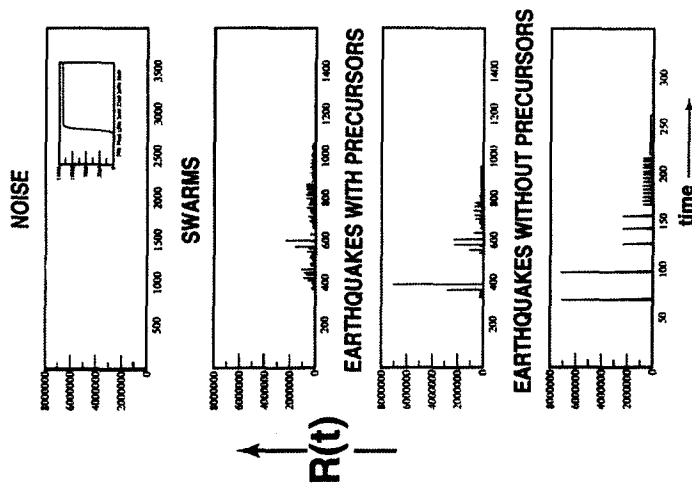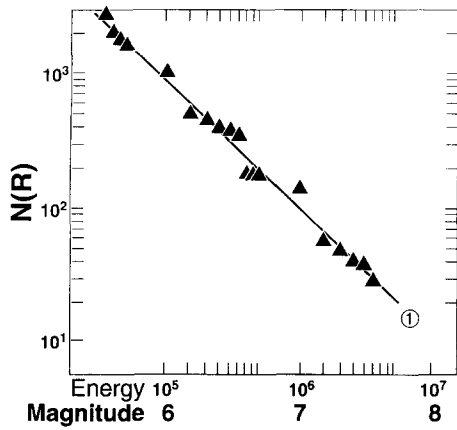
Fig. 8. Simulation of the Gutenberg–Richter law obtained from the summation of different experiments (see main text).

This is absolutely not justified since we take a delay time for distributing energy in the single domain case; this is only to simplify the approach. This point will be implemented in future. Let us write down the equations by considering a transfer of energy associated with $E(t)$ and $R(t)$. The time variation of the energy $E_d(t)$ of domain D_d is given by

$$E_d(t + 1) = E_d(t)(1 - S_d) + \Delta E_d - R_d(t)$$
$$+ \sum_{i \neq d} l_{id} E_i(t) + \sum_{i \neq d} m_{id} R_i(t) \quad (11)$$
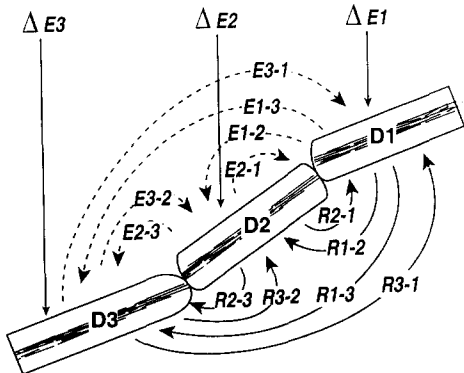
with

$$S_d = \sum_{\substack{i = 1 \\ i \neq d}}^{p} l_{di}$$

Fig. 9. The cartoon shows how the three domains D_1, D_2, D_3 receive and exchange energy in E and R modes and how we define the coefficients of the transfer matrix.

In matrix form

$$E(t + 1) = \Delta \vec{E} + E\vec{E} + (R - I)\vec{R}$$

E, R, I being $(p \times p)$ matrices and $\vec{E}$, $\vec{R}$, $\vec{p}$ dimensional column vectors.

If we suppose that exchanges between domains are limited to adjacent domains, as in Burridge and Knopoff (1967) or Carlson and Langer (1989) models of slider blocks, the transfer matrices E and R are simple band matrices

$$\overline{\overline{E}} = \begin{vmatrix} (1 - S_1) & l_{21} & 0 & 0 & . & 0 \\ l_{12} & (1 - S_2) & l_{32} & 0 & . & 0 \\ 0 & l_{23} & (1 - S_3) & l_{43} & . & 0 \\ . & & . & . & . & . \\ . & & & & & l_{p,p-1} \\ 0 & & & & & (1 - S_p) \end{vmatrix}$$

$$\overline{\overline{R}} = \begin{vmatrix} 0 & m_{21} & 0 & 0 & . & 0 \\ m_{12} & 0 & m_{32} & 0 & . & 0 \\ 0 & m_{23} & 0 & m_{43} & . & 0 \\ . & & . & . & . & . \\ . & & & & & m_{p,p-1} \\ 0 & & & & & 0 \end{vmatrix}$$

We consider the two matrices E and R independent of time. This is a strong simplification, probably acceptable when considering a seismic cycle, but certainly not when considering *a historical or geological sequence of earthquakes*. Let us point out that, since we use a scaling approach here, the formalism can be applied to a sequence of earthquakes over a period of years, an historical study of a large part of a fault zone over periods of hundreds of years, a geological study of the mechanism of generating earthquakes in plate tectonics. The definition of domains, timescales, interaction matrices, merely has to be adapted and scaled to the problem at hand.

2.2.2. Numerical experiments of multidomain cases

For the sake of simplicity, we take the case of only three domains with mutual interactions. The computations can easily be extended to n ($n > 3$) domains. We have carried out several types of

experiments to illustrate the method rather than to build a definitive model.

2.2.2.1. The same ΔE and K for all domains (Fig. 10).

The three domains exchange energy through operators E and R. Let us consider first the symmetrical case where domains D_1 and D_3 are identical and interactions are essentially a transfer of energy from D_1 and D_3 to D_2 (see Fig. 9). We examine successively the case where (D_1, D_2, D_3), when non-interacting, belong to noise, swarms, earthquakes with precursors, and earthquakes without precursors categories.

Fig. 10 shows that, depending on the exchange matrices one can create earthquakes and, more important, generate complex sequences of earthquakes. One case is particularly illustrative: we start from domains of the swarm category (when isolated) and then generate earthquakes in D_2 and noise in D_1 and D_3 when energy is totally transferred to D_2 (Fig. 10(a)). This is a 'focused' case like those studied for the Landers earthquakes by King et al. (1993) using a combination of geological studies and elasticity theory.

Adding a large transfer matrix R generates an earthquake with small precursors in D_1 and D_3 while this earthquake generates in turn an earthquake in D_2, giving as a result a complete sequence (Fig. 10(b)).

An opposite case is when we start with all the domains belonging to the category 'earthquake with precursors' (when isolated); a moderate transfer matrix makes D_2 turn into the large earthquake class and D_1 and D_3 into the swarm class (not shown) etc. Clearly, none of these cases can be predicted easily, and the model displays a clear non-linear behaviour.

2.2.2.2. Different ΔE and K (Fig. 11).

We consider now the case where the domains D_1, D_2, D_3 have different rates of creating microfaults (K) and receive different amounts of energy per unit of time (ΔE). As in the previous experiment, the behaviour of the domains is changed drastically by the interactions. Let us present a few examples to illustrate these changes. We will use the same interaction matrix as in the case of the previous paragraph (the large R matrix). Let us start with

three domains which, when uncoupled, display swarms, earthquakes with precursors, and earthquakes without precursors; after interaction D_1 presents earthquakes without precursors; D_2 is blank, D_3 still has earthquakes but with precursors. We have an exchange of symmetry. The last example may be the most spectacular: the three (isolated) domains have a blank behaviour; large coupling makes D_1 stay blank but D_2 and D_3 behave as earthquakes without precursors. These examples show that the model can generate all kinds of earthquakes sequences.

3. Conclusions

It is clear that our fault model can account correctly for the different type of behaviour observed on a fault prone to earthquakes. It is also clear that our approach is still in many aspects naive; but in this paper we have illustrated a method rather than obtained definitive results. There are a lot of items we intend to tackle in the future.

(1) Transform the probability law (Eq. 3) of creating microfaults from a linear to an exponential one, introducing some kind of barrier energy. A longer quiescence period will result. But, more importantly, such a law will allow us to account for the time-varying relationship between p_1 and e_f: the probability of creating or developing cracks obviously depends on already existing cracks (Sholtz, 1990), and K is certainly an increasing non-linear function of time.

(2) Consider the interaction between cracks with different polarizations as in our previous paper on fracture (Allègre and Le Mouël, 1994); in other words, consider a tensorial stress field rather than the simplified scalar approximation adopted here. A more sophisticated transfer polynomial and more realistic Gutenberg–Richter law will result; the link with the physical world will certainly be stronger but no qualitative change in the behaviour is to be expected. In fact, we could consider a more general transfer polynomial P_k with an expression depending on k, with a renormalization procedure at each step; pro-

vided that the polynomial degree is high enough, the critical behaviour will be respected.

(3) Consider the fault area as a multidomain (with N domains) and introduce delay times in the interactions, especially through the E matrix. This will undoubtedly increase the non-linear characteristics of the system, but also will be closer to reality.

(4) Apply the formalism to a real case as in the King et al. (1993) approach, including the fact that the geometrical motion of the fault can be taken into account by supposing that $R(t)$ and the displacement are proportional. With a realistic geometry of fault, we should be able to reproduce the sequence of aftershocks not only in

time, but also in space (Rundle and Jackson, 1977).

Our approach belongs to the general category of non-linear instability approaches applied to faulting (Keilis-Borok, 1990; Burridge and Knopoff, 1967), with a hierarchical organization of faulting (Scholz, 1982; Narkunskaya and Schnirman, 1990; Turcotte, 1992). But it is also a link between this type of approach and a more physical one like those of Madariaga (1976), Das and Scholz (1981), Lay and Kanamori (1981), and also with the tectonical type of approach (Tapponnier et al., 1990; Stein et al., 1992; Lockner and Byerlee, 1993; King et al., 1993). The approach presented here bridges the gap between elastic the-
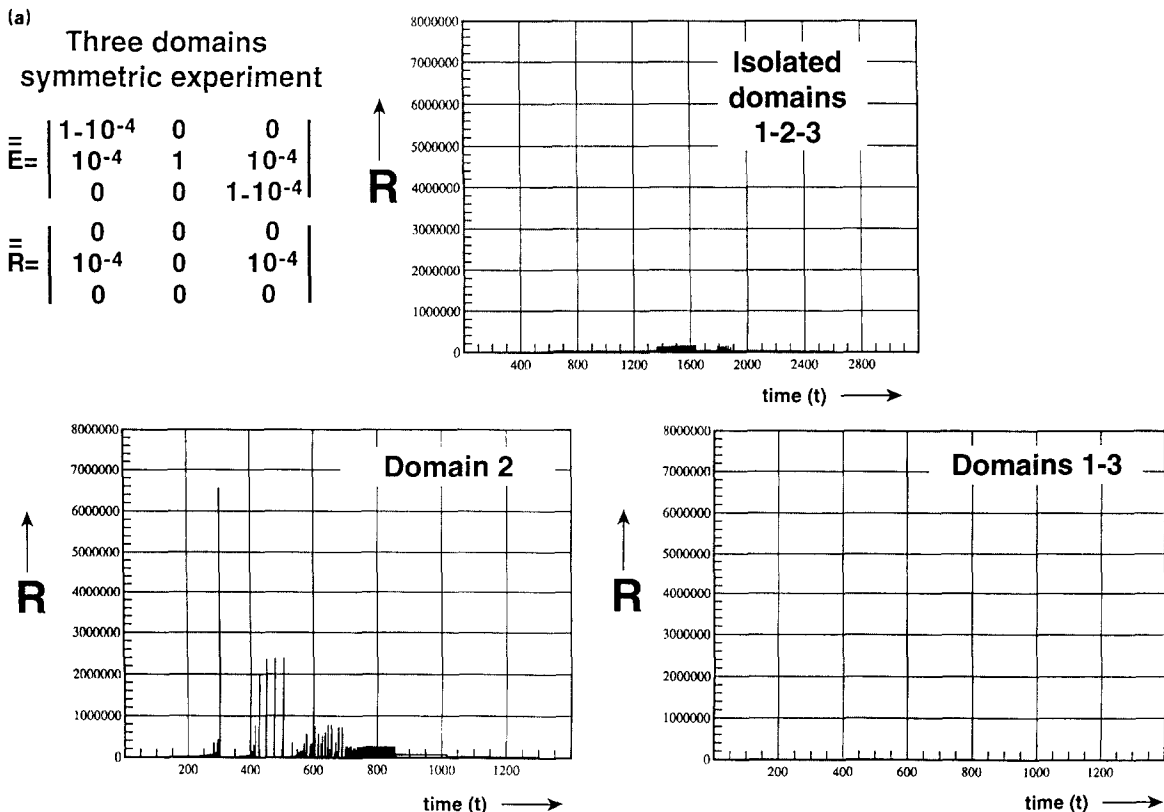

Fig. 10. This is to illustrate the three-domain experiment. D_1, D_2, D_3 receive the same energy and have the same K. (a) D_1, D_2 and D_3, when non-interacting, are in the little swarms domain. D_1 and D_3 transfer energy to D_2 with the same transfer matrix: (Large E, small R; the result is to create earthquakes in D_2. This is a kind of focused energy case like that studied by Stein et al. (b) Same domains D_1, D_2, D_3 as in (a), when isolated. However, the transfer matrix R is different, it is now large and symmetrical. D_2 transfers energy also to D_1 and D_3 through the R matrix. Two sets of large earthquakes are generated.

(b)

Three domains
symmetric experiment

$$\overline{\overline{E}} = \begin{vmatrix} 1\text{-}10^{-4} & 0 & 0 \\ 10^{-4} & 1 & 10^{-4} \\ 0 & 0 & 1\text{-}10^{-4} \end{vmatrix}$$

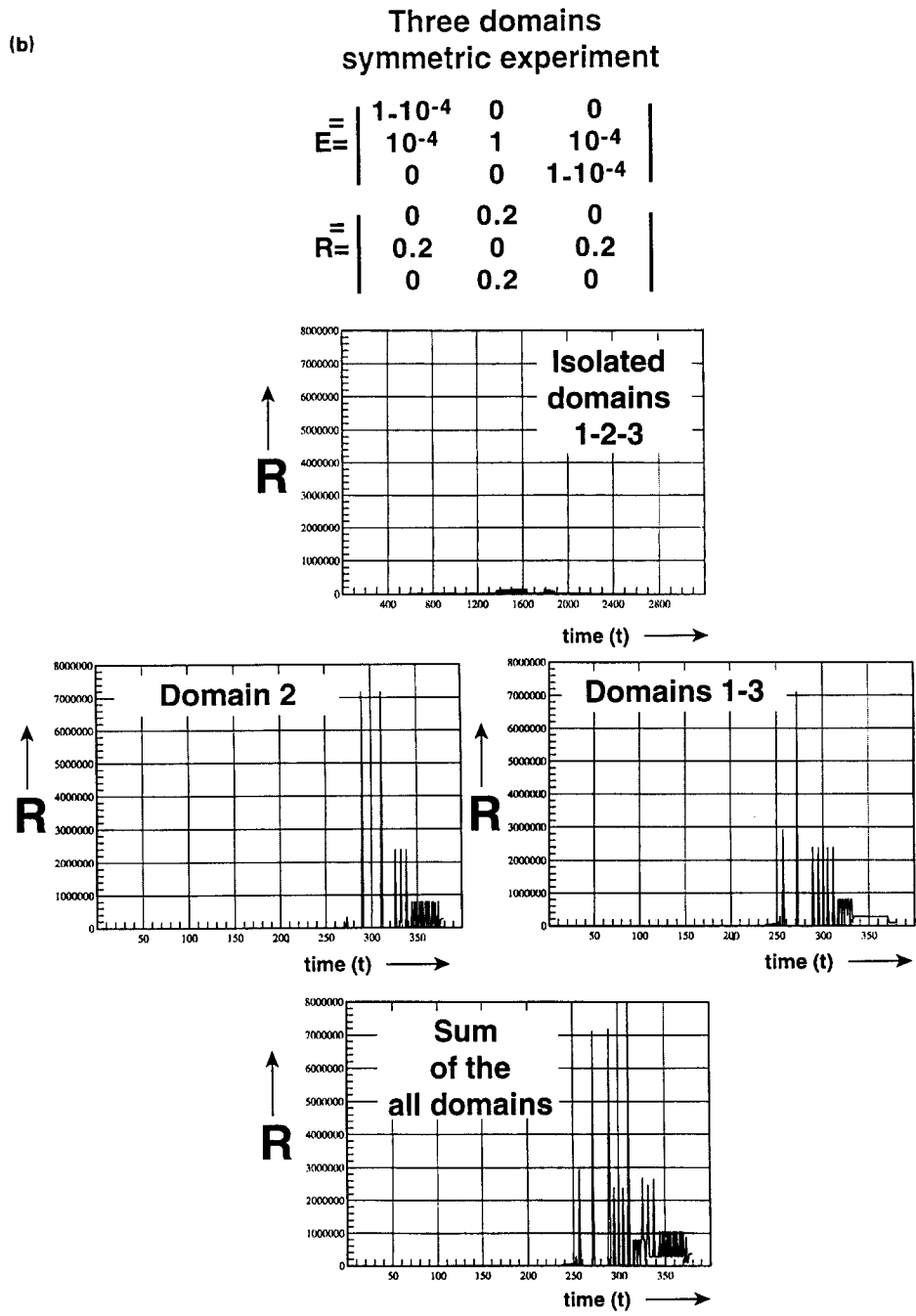$$\overline{\overline{R}} = \begin{vmatrix} 0 & 0.2 & 0 \\ 0.2 & 0 & 0.2 \\ 0 & 0.2 & 0 \end{vmatrix}$$

Fig. 10 (continued).

ory of rupture, non-linear dynamics and scaling laws: energy considerations bridge the gap between physical elasticity and scaling techniques while the mulitdomain case provides a link between the Burridge–Knopoff approach and scaling technics. Overall, our approach fits the funda-

Three domains experiments

(a)

$$\underset{=}{\equiv}E=\begin{vmatrix} 1\text{-}15\ 10^{-4} & 10^{-4} & 5\ 10^{-4} \\ 10^{-4} & 1\text{-}2\ 10^{-4} & 10^{-4} \\ 5\ 10^{-4} & 1\text{-}15\ 10^{-4} \end{vmatrix}$$

$$\underset{=}{\equiv}R=\begin{vmatrix} 0 & 0.2 & 0.1 \\ 0.2 & 0 & 0.2 \\ 0.1 & 0.2 & 0 \end{vmatrix}$$

Domain 1
$\Delta E=5\ 10^3$
$K=8\ 10^{-7}$

Domain 2
$\Delta E=2\ 10^4$
$K=3\ 10^{-7}$

Domain 3
$\Delta E=8\ 10^4$
$K=5\ 10^{-7}$

Domain (1)
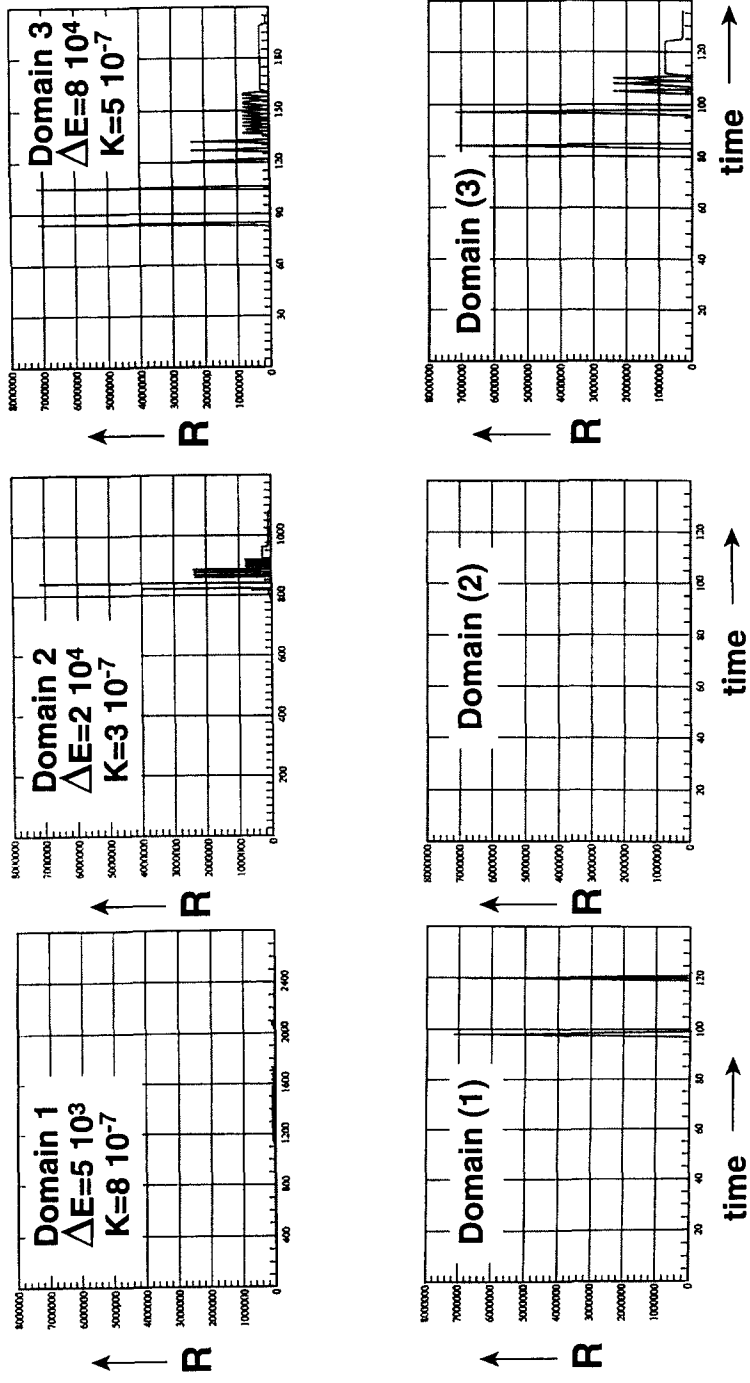
Domain (2)

Domain (3)

Fig. 11. The three domains have different ΔE and K. (a) The three isolated domains behave, respectively, as swarms, earthquakes with precursors, earthquakes without precursors. Through the large R transfer matrix, focusing on domains D_1 and D_3 generates earthquakes without precursors. (b) The three isolated domains are blank. Through a large and dissymetrical R, earthquakes are generated in D_2 and D_3.

Three domains experiments

‖E=	1-2 10⁻⁴	10⁻⁴	10⁻⁴
	10⁻⁴	1-2 10⁻⁴	10⁻⁴
	10⁻⁴	10⁻⁴	1-2 10⁻⁴

‖R=	0	0.6	0.2
	0.6	0	0.2
	0.2	0.2	0

Domain 1
ΔE=3 10³
K=2 10⁻⁷

Domain 2
ΔE=8 10³
K=5 10⁻⁷

Domain 3
ΔE=2 10³
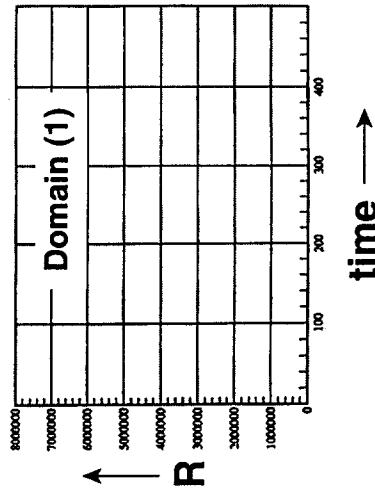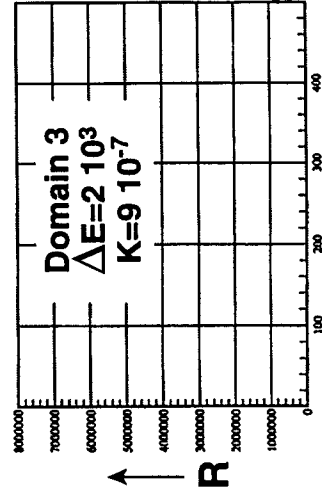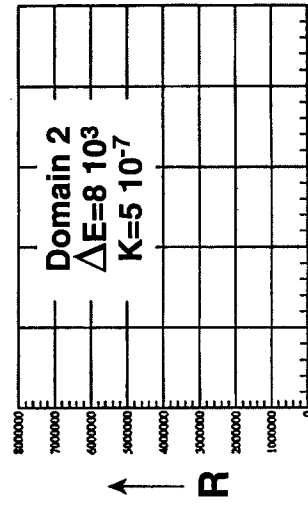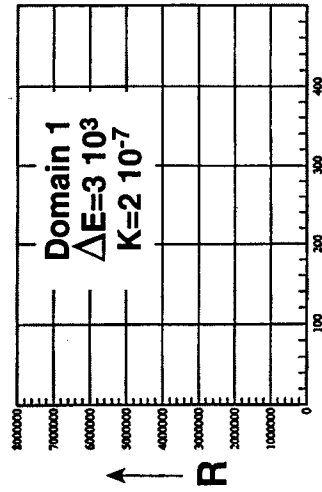K=9 10⁻⁷

Domain (1)

Domain 2

Domain (3)

Fig. 11 (continued).

(b)
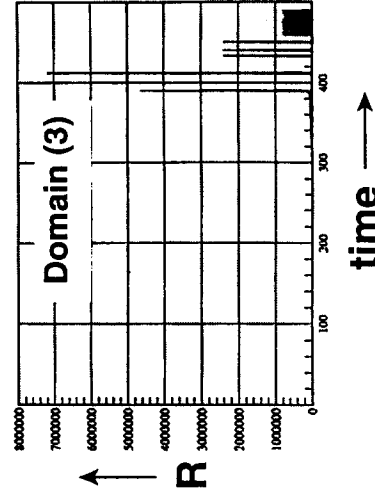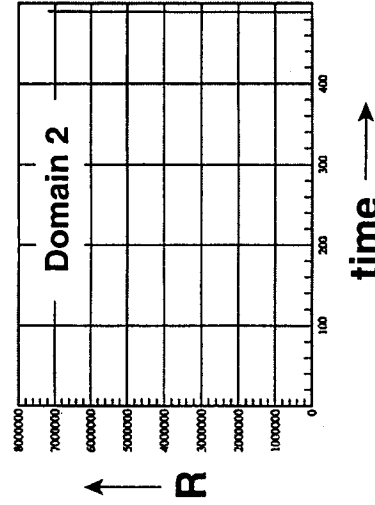
mental observation that earthquakes, tectonics and faulting have scaling characteristics.

References

Aki, K. 1967. Scaling low of seismic spectrums. J. Geophys. Res., 72:1217–1231.

Aki, K., 1984. Asperities, barriers, characteristic earthquakes and strong motion prediction. J. Geophys. Res., 86: 5867–5872.

Aki, K., 1987. Magnitude–frequency relation for small earthquakes; a clue to the origin of f_{max} of large earthquakes. J. Geophys. Res., 92: 1349–1355.

Allègre, C.J. and Le Mouël, J.L., 1994. Introduction of scaling technique in brittle fracture of rocks. Phys. Earth Planet. Inter., 87: 85–93.

Allègre, C.J., Le Mouël, J.L. and Provost, A., 1982. Scaling rules in rock fracture and possible implications for earthquake prediction. Nature, 297: 47–49.

Ambrayseys, N., 1970. Some characteristic fractures of the Anatolian zone. Tectonophysics, 9: 143–165.

Armijo, R., Tapponnier, P. and Tonglin, H., 1989. Late Cenozoic right-lateral strike–slip faulting in southern Tibet. J. Geophys. Res., 94: 2787–2839.

Brace, W.F. and Bombolakis, A.G., 1963. A note on brittle crack growth in compression. J. Geophys. Res., 68: 3709–3713.

Brace, W.F., Paulding, B.W. and Scholz, C.H., 1966. Dilatancy in the fracture of crystalline rocks. J. Geophys. Res., 71: 1939.

Burridge, R. and Knopoff, L., 1967. Model and theoretical seismicity. Bull. Seismol. Soc. Am., 57: 341–371.

Carlson, J.M. and Langer, J.S., 1989. Mechanical model of an earthquake fault. Phys. Res. A., 40: 6470–6484.

Chelidze, T.L., 1982. Percolation and fracture. Phys. Earth Planet. Inter., 28: 93–101.

Das, S. and Aki, K., 1977. Fault plane with barriers: a versatile earthquake model. J. Geophys. Res., 82: 5658–5670.

Das, S., and Scholz, C., 1981. Theory of time-dependent rupture in the earth. J. Geophys. Res., 86: 6039–6051.

Gutenberg, B. and Richter, F., 1954. Seismicity of the Earth and Associated Phenomenon, 2nd edn. Princeton University.

Hanks, T., 1977. Earthquake stress drops, ambient tectonic stress and stresses that drive plates. Pure. Appl. Geophys., 115: 441–458.

Hirata, T., 1989. Fractal dimension of fault system in Japan. Fractal structures in rock fractures geometries at various scales. Pure Appl. Geophys., 131: 157–170.

Kanamori, H., 1980. The state of stress in the Earth's lithosphere. Physics of the Earth's interior. Corso, 78: 531–554.

Kanamori, H. and Anderson, D.L., 1975. Theoretical basis of some empirical relations in seismology. Bull. Seismol. Soc. Am., 65: 1073–1096.

Keilis-Borok, V.I., 1990. The lithosphere of the Earth as a non-linear system with implications for earthquakes predictions. Rev. Geophys. Res., 28: 9–34.

King, G., 1983. The accommodation of large strain in the upper lithosphere of the earth and other solids by self similar fault systems. The geometrical origin of b. values. Pure. Appl. Geophys., 121: 761–815.

King, G.C.P., Stein, R.S. and Rundle, J.B., 1988. The growth of geological structures by repeated earthquakes: conceptual framework. J. Geophys. Res., 93: 13 307–13 318.

King, G.C.P., Stein, R.S. and Jian, L., 1993. Static stress changes and the triggering of earthquakes. Bull. Seismol. Soc. Am., 84: 935–953.

Lay, T. and Kanamori, H., 1981. An asperity model of great earthquake sequences. In D. Simpson and P. Richard (Editors) Earthquake Prediction, an International Review. M. Ewing Ser 4. Am. Geophys. Union, Washington, DC, pp. 579–592.

Lockner, D. and Byerlee, J., 1993. How geometrical constraints contribute to the weakness of nature fault. Nature. 363: 250–252.

Madariaga, R., 1976. Dynamics of an expanding circular fault. Bull. Seismol. Soc. Am., 66: 636–666.

Mattauer, M., 1976. Les Déformations de l'Écorce Terrestre. Hermann, Paris.

Narkunskaya, G.S. and Schnirman, M.G., 1990. Hierarchical model of defects development and seismicity. Phys. Earth Planet. Inter., 61: 29–35.

Newman, W.I., Gabrielov, A., Durand, T.A., Phoenix, S.L. and Turcotte, D.L., 1993. An exact renormalization model for earthquakes and material failure: statics and dynamics. Technical Rep. 93–69, Mathematical Sciences Institute, Cornell University.

Otsuka, M., 1972. A chain reaction type source model a a tool to interpret the frequency–magnitude relation of earthquakes. J. Phys. Earth., 20: 35–45.

Rundle, J.B. and Jackson, D.D., 1977. Numerical simulation of earthquake sequences. Bull. Seismol. Soc. Am., 67: 1363–1377.

Sammis, C.G., Osborn, R.H., Anderson, J.L., Banerdt, M. and White, P., 1986. Self similar cataclasis in the formation of fault gouge. Pure. Appl. Geophys., 123: 53–78.

Scholz, C., 1982. Scaling laws for large earthquakes: consequences for physical models. Bull. Seismol. Soc. Am., 72: 1–14.

Scholz, C., 1990. The Mechanics of Earthquake and Faulting. Cambridge University.

Smalley, R.J., Turcotte, R.J. and Solla, D.L., 1985. A renormalization group approach to the stick-slip behaviour of faults. J. Geophys. Res., 90: 1894–1900.

Stein, R., King, G. and Jianlin, C.P., 1992. Change in failure stress on the Southern San Andreas fault system caused by the 1992 magnitude = 7.4 Landers earthquake. Science, 258: 1328–1332.

Tapponnier, P. and Brace, W.F., 1976. Development of stress-induced microcracks in Westerly granite. Int. J. Rock Mech. Min. Sci. Geomech abstr., 13: 103–112.

Tapponnier, P., Meyer, B., Avouac, J.P., Peltzer, G., Gaudemer, Y., Shunnin, G., Hongfa, X., Kelun, Y., Zhitai, C., Shuahua, C. and Huagang, D., 1990. Active thrusting and folding in the Qilian Shan, and decoupling between upper crust and mantle in northeastern Tibet. Earth Planet. Sci. Lett., 97: 382–403.

Turcotte, D.L., 1992. Fractals and Chaos in Geology and Geophysics. Cambridge University.

Wilson, K.G., 1979. Problems in physics with many scales of length. Sci. Am. August, 140–157.